

Complex shape evolution of electromigration-driven single-layer islands

Philipp Kuhn,^{1,2} Joachim Krug,^{2,*} Frank Hausser,³ and Axel Voigt³

¹*Fachbereich Physik, Universität Duisburg-Essen, 45117 Essen, Germany*

²*Institut für Theoretische Physik, Universität zu Köln, Zùlpicher Strasse 77, 50937 Köln, Germany*

³*Crystal Growth group, research center caesar, Ludwig-Erhard-Allee 2, 53175 Bonn, Germany*

(Dated: March 30, 2018)

The shape evolution of two-dimensional islands through periphery diffusion biased by an electromigration force is studied numerically using a continuum approach. We show that the introduction of crystal anisotropy in the mobility of edge atoms induces a rich variety of migration modes, which include oscillatory and irregular behavior. A phase diagram in the plane of anisotropy strength and island size is constructed. The oscillatory motion can be understood in terms of stable facets which develop on one side of the island and which the island then slides past. The facet orientations are determined analytically.

PACS numbers: 68.65.-k, 66.30.Qa, 05.45.-a, 85.40.-e

The manipulation of nanostructures by macroscopic forces is likely to become a key ingredient in many nanotechnology applications. Understanding the influence of external fields on the shape evolution of nanoscale surface features is therefore of considerable importance. As a first step in this direction we analyze here the effects of an electric current on single-layer islands on a crystalline surface. The islands evolve under surface electromigration, the directed motion of adsorbed atoms due to the slight force transmitted by collisions with the conduction electrons in the sample [1].

Electromigration along interfaces and grain boundaries is the most persistent and menacing reliability problem in integrated circuit technology [2, 3]. Correspondingly, much work has been devoted to electromigration-induced void formation and breakdown in metallic conductor lines [3], and the capacity for quantitative numerical modeling has been demonstrated at least for simple void geometries [4, 5]. A major obstacle to achieving predictive power in such studies, however, is the insufficient control over the complex internal structure of the polycrystalline samples. Hence an important motivation for investigating electromigration-induced effects on simple, well-controlled nanoscale morphologies, such as step patterns on vicinal surfaces [6] and single layer islands [7], is to bridge the gap between the microscopic mechanisms of electromigration and their consequences on technologically relevant length and time scales.

Electromigration of islands has been modeled previously using Monte Carlo simulations [8] and continuum theory [9]. The continuum approach to island shape evolution, which treats the island edge as a smooth curve, has been successfully applied to a range of problems including the diffusion [10] and sintering [11] of islands, and the pinch-off of vacancy clusters [12]. Here we focus on the regime of periphery diffusion (PD), where the dominant kinetic process is the migration of atoms along the island boundary. The shape then follows a local evolution law, without coupling to the adatom concentration

on the surrounding terrace.

We extend the model of [9] by including crystal anisotropy in the adatom mobility. It was observed recently in the context of step flow growth [13] that crystalline anisotropy can change the behavior of step patterns in a *qualitative* way. In the present case, it leads to the unfolding of a remarkable richness of dynamic phenomena: In addition to the scenarios of steady motion and island breakup [5, 9] observed in previous work, we find spontaneous symmetry breaking, oscillatory shape evolution, and complex migration trajectories where different modes of motion alternate in a periodic or irregular fashion. This highlights the importance of properly including anisotropy in the modeling of boundary evolutions. Oscillatory shape dynamics has been seen previously in a numerical study of void electromigration [14], and transitions to quasiperiodicity and chaos are known to occur in directional solidification [15, 16]. To the best of our knowledge, however, our work provides the first example of complex shape evolution for a *closed* contour subject to purely *local* dynamics.

In the PD regime, the normal velocity v_n of the island boundary satisfies the continuity equation

$$v_n + \frac{\partial}{\partial s} \Omega \sigma \left[-\frac{\partial}{\partial s} (\Omega \tilde{\gamma} \kappa) + q^* E_t \right] = 0. \quad (1)$$

Here s denotes the arclength along the island edge, and Ω the atomic area. The square bracket multiplied by the edge atom mobility σ is the total mass current along the boundary, which is driven by the tangential derivative of the chemical potential $\Delta\mu = \Omega \tilde{\gamma} \kappa$ and the electromigration force $q^* E_t$; $\tilde{\gamma}$ is the edge stiffness, κ the local curvature, q^* the effective charge of an edge atom, and E_t the tangential component of the local electric field. The crystal anisotropy of the surface enters through the dependence of $\tilde{\gamma}$ [17] and σ [11, 18] on the orientation angle θ of the island edge.

For atomic layer height islands on the surface of a thick sample, the island boundary has a negligible effect on the

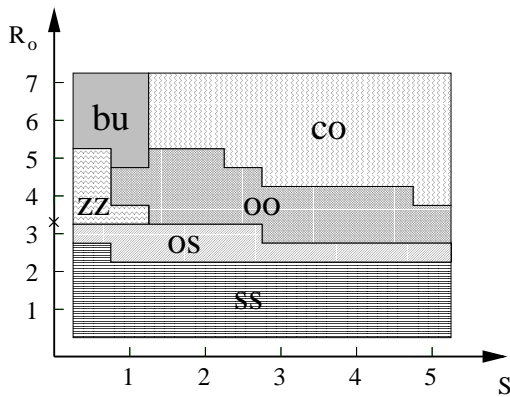


FIG. 1: Phase diagram of migration modes in the plane of anisotropy strength S and island radius R_0 , for sixfold anisotropy ($n = 6$) and the field aligned with a direction of maximal mobility ($\alpha = 0$). For each point on a grid of resolution 0.5×0.5 , the evolution of the island was followed until the asymptotic mode could be identified. We distinguish between straight stationary (ss), oblique stationary (os), oblique oscillatory (oo), zigzag (zz) and complex oscillatory (co) motion. In the region **bu** islands break up. The cross on the R_0 -axis indicates the linear instability of the circular solution in the isotropic case.

electric field; this is in contrast to the modeling of voids in conductor lines, where the coupling of the void shape to the electric field leads to a manifestly nonlocal problem [4, 5, 14]. Here we can take the field to be of constant strength E_0 and aligned along the x -axis. Letting θ denote the angle between the normal of the island edge and the y -axis (counted positive in the clockwise direction), this implies $E_t = E_0 \cos(\theta)$.

Together with the specification of $\tilde{\gamma}$ and σ , to be addressed below, this completes the definition of the local boundary evolution (1). Comparing the two terms inside the square brackets, we extract the characteristic length scale [5, 9, 19] $l_E = \sqrt{\Omega \tilde{\gamma} / |q^* E_0|}$, which gauges the relative importance of capillary and electromigration forces; electromigration dominates on scales large compared to l_E . Below all lengths are reported in units of l_E .

The isotropic version of (1), with $\tilde{\gamma}, \sigma = \text{const.}$, has been studied previously by Suo and collaborators [19, 20, 21]. A circular island moving at constant velocity is stable for (dimensionless) radii $R < R_c \approx 3.26$ [21]. Beyond the instability a bifurcation to two branches of non-circular stationary solutions occurs [20]. Numerical integration of the time-dependent problem [22] shows that only one of the branches, corresponding to islands elongated in the field direction, is realized. At large radii island breakup occurs, mediated by the outgrowth of a finger of the kind found in [19].

We now turn to the effects of crystal anisotropy. Throughout this paper only the anisotropy of the adatom mobility σ will be taken into account, while the edge stiffness $\tilde{\gamma}$ is kept isotropic. This is motivated partly by the

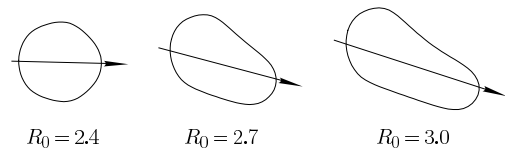


FIG. 2: Stationary shapes for $S = 2$ near the transition from **ss** to **os** behavior. Arrows indicate the direction of motion.

fact that the anisotropy in σ is found experimentally (to the extent that it has been investigated) to much exceed that of $\tilde{\gamma}$ [18], and partly by our desire to disentangle kinetic (σ) and thermodynamic ($\tilde{\gamma}$) effects [23]. For the kinetic anisotropy we employ the functional form [5]

$$\sigma(\theta) = \sigma_{\max}(1 + S)^{-1} \{1 + S \cos^2[n(\theta + \alpha)/2]\}. \quad (2)$$

Since the prefactor σ_{\max} only sets the time scale, the relevant parameters in (2) are the anisotropy strength S , the number of symmetry axes n , and the angle α between the symmetry axes and the electric field direction. The natural time unit is $t_E = l_E^4 / (\sigma_{\max} \tilde{\gamma} \Omega^2)$ [5].

The simplest solutions in the anisotropic case are stationary islands moving at constant speed, which satisfy the equation $v_n = V \sin(\theta + \phi)$; here the angle ϕ accounts for the fact that the island does not necessarily move in the field direction. A complete analysis of stationary island shapes has been achieved in the limiting case of zero stiffness [22]. For an even number n of symmetry axes smooth stationary shapes are found for small S , while for larger anisotropy the shapes develop self-intersections; no stationary shapes exist when n is odd. The migration direction generally lies between the field direction and the symmetry axis of the anisotropy.

Despite their mathematical interest, these results are of limited applicability to real islands, because all stationary shapes are wildly unstable when $\tilde{\gamma} = 0$. In the remainder of the article we therefore focus on the numerical solution of the full, time-dependent problem with $\tilde{\gamma} > 0$ and $\sigma(\theta)$ given by (2). Two complementary numerical algorithms have been employed. For relatively small islands a finite difference scheme described in [5] was found to be most efficient, while for large islands we rely on the better stability properties of a semi-implicit adaptive finite element algorithm. [24]. The full mutual consistency of the two approaches has been checked.

Most results have been obtained for $n = 6$ and $\alpha = 0$. This leaves the anisotropy strength S and the initial condition for the deterministic shape evolution to be specified. Extensive calculations show that the dependence on the precise initial shape is minor [25], and hence the initial condition can be characterized by the radius R_0 of a circular island of the same area; in practice, we usually start the calculation from a slightly distorted circle.

The phase diagram in Fig.1 gives an overview of the observed migration modes in the $S - R_0$ -plane [26]. For small islands ($R_0 \leq 2$) the evolution converges to a sta-

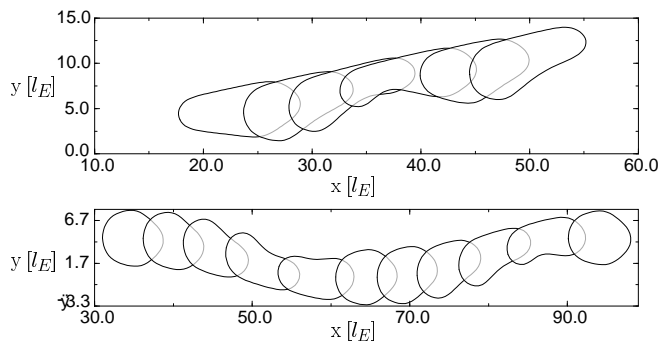


FIG. 3: Snapshots of **oo** motion for $R_0 = 4$ and $S = 1$ (upper panel) and **zz** motion for $R_0 = 3.5$, $S = 0.5$ (lower panel), taken at time intervals $\Delta t = 20$. In both cases the perimeter displays simple oscillations, as in the bottom panel of Fig.4.

tionary shape which moves in the direction of the field. For large S the shapes develop facets [22], similar to what has been observed for void electromigration [5]. Increasing the island radius the direction of migration starts to deviate from the field direction, and we enter the regime of oblique stationary (**os**) motion (Fig.2). Since the field is aligned with the symmetry axis of the anisotropy, the appearance of obliquely moving solutions implies that the symmetry of the problem is *spontaneously* broken. In the **os** regime, pairs of symmetry-related stationary solutions coexist; which solution is chosen in a given run depends on the initial condition.

Upon further increase of R_0 the obliquely moving shapes start to oscillate (Fig.3). Near the onset of oblique oscillatory (**oo**) motion at radius R_0^c the oscillation period diverges as $T \sim |R_0 - R_0^c|^{-\nu}$ with $\nu \approx 2.5$. For larger radii higher harmonics of the fundamental oscillation period appear and the motion becomes increasingly irregular (Fig.4). This characterizes the complex oscillatory (**co**) regime, which is exemplified in Fig.5. The direction of island motion displays random shifts, which seem to be triggered by small fluctuations. This behavior is typical for large islands, and it is distinct from the *periodic* direction changes seen in the zig-zag (**zz**) regime for moderate sizes and small anisotropies (Fig.3).

The true long time behavior for large islands ($R_0 > 7$) and large anisotropy ($S > 5$) could not be pinned down unambiguously with our current numerical methods. Generally speaking, large islands with small anisotropy break up, while for large R_0 and S faceted shapes undergoing irregular motion dominate.

The example shown in Fig.5 provides an important clue to the origin of the complex shape evolution. After an initial transient lasting until $t \approx 300$, the island settles down into a shape consisting of a straight upper edge and a lower edge which has broken up into a faceted hill-and-valley structure. The direction of island motion coincides with the orientation of the upper, straight edge, as shown for a smaller island in the upper panel of Fig.3. The key

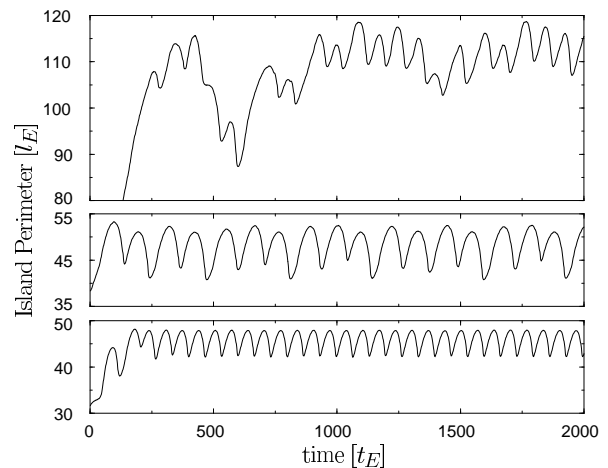


FIG. 4: Time series of the island perimeter showing regular and irregular oscillations. From bottom to top the parameters are $S = 2, R_0 = 5$; $S = 5, R_0 = 5$; and $S = 3, R_0 = 8$. The top panel corresponds to the run shown in Fig.5.

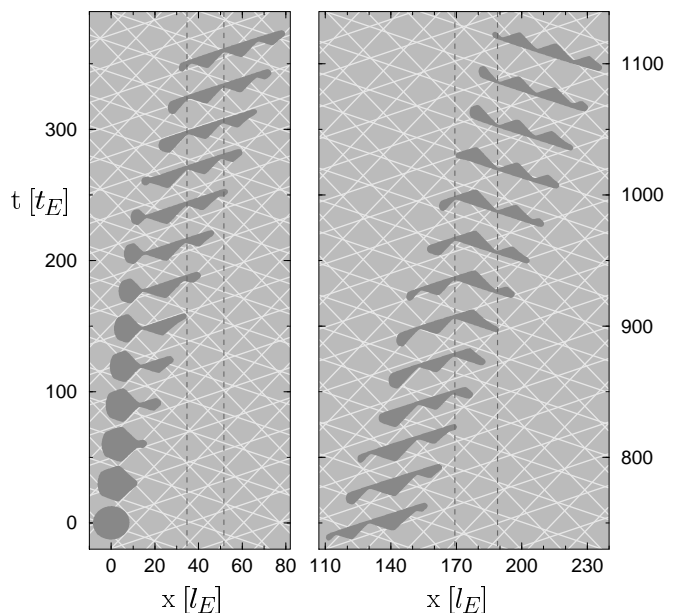


FIG. 5: Complex oscillatory motion with $S = 3$, $R_0 = 8$. Light lines show the facet orientations predicted from (3), dark dashed lines illustrate that the hill-valley structure is static in the substrate frame. Consecutive snapshots are shifted upwards in time.

observation is that the hill-and-valley structure on the faceted edge *does not* move in the substrate frame. The moving island slides past the static facets, causing the shape to oscillate. Around $t \approx 900$ the roles of the upper and lower edges are seen to reverse, and the direction of motion changes.

Quite generally, large islands in the **co** regime can be constructed from four selected facet orientations $\theta_1, \theta_2, \theta_3, \theta_4$. Here θ_1 and θ_2 are the possible stable orientations of the upper island edge, which must satisfy

$-\pi/2 < \theta_1 < 0 < \theta_2 < \pi/2$. In the case considered here ($\alpha = 0$, n even) the corresponding orientations θ_3 and θ_4 for the lower edge are obtained by reflection at the x -axis, $\theta_3 = -\pi - \theta_1$ and $\theta_4 = \pi - \theta_2$. To form a closed shape, at least three orientations must be combined, two of which are those two symmetry-related orientations that are closest to the horizontal direction ($\theta = 0$ or π). In Fig.5 we see a transition from a shape with orientations $\{\theta_1, \theta_3, \theta_4\}$ to a shape with orientations $\{\theta_1, \theta_2, \theta_3\}$.

The stable facet orientations can be computed along the lines of [27]. The condition $v_n = 0$ for a static shape implies that the current in (1) is set to a constant j^* . Using the relation $\kappa = d\theta/ds$ this can be brought into the form

$$\Omega\tilde{\gamma}\frac{d^2}{ds^2}\theta = -[j^*/\sigma(\theta) - q^*E_0\cos(\theta)] \equiv -V'(\theta), \quad (3)$$

which describes the position $\theta(s)$ of a particle moving in time s subject to a potential $V(\theta)$ determined by the mobility and the electric field strength. As explained in [27], the coexistence of two stable facet orientations corresponds to a particle trajectory moving between two degenerate potential maxima. To determine the selected orientations, j^* is tuned until two degenerate maxima satisfying the above constraints appear. We have checked that this procedure correctly accounts for the facet orientations observed in the time-dependent calculations throughout the relevant region of the phase diagram (see Fig.5). In general, stable facets can be constructed from (3) only when the anisotropy is sufficiently large [27]. For $n = 6$, $\alpha = 0$ the requirement is $S > S_c \approx 1.77$. No stable facets are found when the number of symmetry axes is too small ($n \leq 3$); this may explain why we do not see oscillatory shape evolution for a threefold anisotropy.

We close with two remarks concerning future research. First, we note that the observed island shapes are quite smooth, which implies that the number of circular harmonics involved in the shape evolution is small. It thus seems promising to attempt a description in terms of a low-dimensional dynamical system, in the spirit of [16], to gain a deeper understanding of the various migration modes and the bifurcations connecting them.

Second, we address the experimental conditions under which the predictions of this paper could be realized. As an example, we consider islands on Cu(100), for which most material parameters entering the theory are available. Following [8], we estimate that the electromigration force on an edge atom at a current density of 10^7 Acm^{-2} is about 400 eV/cm. Together with the experimentally determined stiffness [17] and mobility [18] for kinked steps at 300 K, this yields a characteristic length of $l_E \approx 25$ nm, and a time scale t_E on the order of seconds. Thus we expect complex shape dynamics to be observable for island radii around 100 nm and on time scales of a few hundred seconds. As a first step towards a more detailed description of specific surfaces, it would

be important to identify oscillatory shape evolution in kinetic Monte Carlo simulations of island electromigration.

This work was supported by DFG within SFB 616 *Energy dissipation at surfaces* and SFB 611 *Singular phenomena and scaling in mathematical models*.

* krug@thp.uni-koeln.de

- [1] R.S. Sorbello, Solid State Phys. **51**, 159 (1998).
- [2] Z. Suo, in: *Comprehensive Structural Integrity*, Vol. 8: *Interfacial and Nanoscale Failure*, W. Gerberich, W. Yang, Eds. (Elsevier, Amsterdam 2003), p. 265.
- [3] K.N. Tu, J. Appl. Phys. **94**, 5451 (2003).
- [4] M.R. Gungor, D. Maroudas, J. Appl. Phys. **85**, 2233 (1999).
- [5] M. Schimschak, J. Krug, J. Appl. Phys. **87**, 695 (2000).
- [6] K. Yagi, H. Minoda, M. Degawa, Surf. Sci. Rep. **43**, 45 (2001).
- [7] J.-J. Métois, J.-C. Heyraud, A. Pimpinelli, Surf. Sci. **420**, 250 (1999); A. Saúl, J.-J. Métois, A. Ranguis, Phys. Rev. B **65**, 075409 (2002).
- [8] H. Mehl, O. Biham, O. Millo, M. Karimi, Phys. Rev. B **61**, 4975 (2000).
- [9] O. Pierre-Louis, T.L. Einstein, Phys. Rev. B **62**, 13697 (2000).
- [10] S. V. Khare, N. C. Bartelt, T. L. Einstein, Phys. Rev. Lett. **75**, 2148 (1995).
- [11] D.-J. Liu, J.W. Evans, Phys. Rev. B **66**, 165407 (2002).
- [12] W.W. Pai *et al.*, Phys. Rev. Lett. **86**, 3088 (2001)
- [13] G. Danker, O. Pierre-Louis, K. Kassner, C. Misbah, Phys. Rev. E **68**, 020601(R) (2003).
- [14] M.R. Gungor, D. Maroudas, Surf. Sci. **461**, L550 (2000).
- [15] K. Kassner, C. Misbah, H. Müller-Krumbhaar, Phys. Rev. Lett. **67**, 1551 (1991).
- [16] A. Valance, K. Kassner, C. Misbah, Phys. Rev. Lett. **69**, 1544 (1992).
- [17] S. Dieluweit, H. Ibach, M. Giesen, T.L. Einstein, Phys. Rev. B **67**, 121410 (2003).
- [18] M. Giesen, S. Dieluweit, J. Mol. Cat. A **216**, 263 (2004).
- [19] Z. Suo, W. Wang, M. Yang, Appl. Phys. Lett. **64** 1944 (1994).
- [20] W. Yang, W. Wang, Z. Suo, J. Mech. Phys. Solids **42** 897 (1994).
- [21] W. Wang, Z. Suo, T.-H.Hao, J. Appl. Phys. **79**, 2394 (1996).
- [22] P. Kuhn, J. Krug, in *Multiscale modeling of epitaxial growth*, ed. by A. Voigt, ISNM Vol. 149 (Birkhäuser, 2005), p. 159.
- [23] Preliminary numerical calculations indicate that the scenarios described here are largely preserved in the presence of an anisotropic stiffness (F. Hausser, unpublished).
- [24] E. Bänsch, F. Hausser, A. Voigt, SIAM J. Sci. Comp. (in press).
- [25] In some cases, however, an elongated initial shape can be stabilized for island sizes where a more circular initial condition leads to breakup.
- [26] Similar migration modes have been observed for $n = 4$ and for $n = 6$ with other values of α , with the exception of the case $n = 6$ and $\alpha = \pi/6$, where only straight moving stationary shapes are observed.
- [27] J. Krug, H.T. Dobbs, Phys. Rev. Lett. **73**, 1947 (1994).